

# Chemical Shift Anisotropy as a Mechanism for Modulating Apparent $J_{\text{Tl-H}}$ and $J_{\text{Tl-C}}$ Coupling Constants in Tris(pyrazolyl)hydroborato Thallium Complexes

Prasenjit Ghosh, Peter J. Desrosiers\*,<sup>†</sup> and Gerard Parkin\*

Contribution from the Department of Chemistry, Columbia University, New York, New York 10027

Received May 11, 1998

**Abstract:** Nuclear relaxation due to chemical shift anisotropy provides an efficient mechanism for modulating apparent  $J_{\text{Tl-H}}$  and  $J_{\text{Tl-C}}$  coupling constants in tris(pyrazolyl)hydroborato complexes,  $\text{Tl}[\text{Tp}^{\text{RR}'}]$ . Specifically, thallium relaxation via chemical shift anisotropy results in apparent coupling constants to thallium being dramatically reduced at (i) higher applied magnetic field strengths and (ii) lower temperatures. As a result of this phenomenon, the absence of observable  $J_{\text{Tl-H}}$  and  $J_{\text{Tl-C}}$  coupling constants, per se, should not be taken as definitive evidence that either (i) the structure is static with a coupling constant of zero or (ii) dissociation of Tl is rapid on the NMR time scale, thereby resulting in an observed loss of coupling.

## Introduction

Trofimenko's tris(pyrazolyl)hydroborato ligand system,  $[\text{Tp}^{\text{RR}'}]$ , is one of the most versatile and widely used in modern coordination chemistry.<sup>1,2</sup> In particular, thallium complexes,  $\text{Tl}[\text{Tp}^{\text{RR}'}]$  (Figure 1), have played a prominent role as reagents in the development of this chemistry, with the consequence that a large variety of these derivatives has been investigated by X-ray diffraction and NMR spectroscopy.<sup>3</sup> The latter technique has been used to infer both structural and dynamic differences between various  $\text{Tl}[\text{Tp}^{\text{RR}'}]$  derivatives.<sup>4–11</sup> For example, the observation that  $J_{\text{Tl-C}}$  coupling constants for  $\text{Tl}[\text{Tp}^{\text{Bu}^t, \text{Me}}]$ <sup>4</sup> are

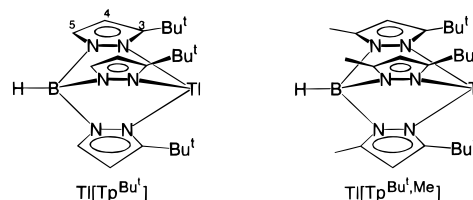


Figure 1.  $\text{Tl}[\text{Tp}^{\text{RR}'}]$  complexes.

greater than the corresponding values in  $\text{Tl}[\text{Tp}^{\text{Bu}^t}]$ <sup>12</sup> has been attributed to repulsions between the 5-methyl substituents forcing the 3-*tert*-butyl groups closer to the thallium nucleus;<sup>4,13</sup> likewise, the broad nature of the 9-H proton resonance in  $\text{Tl}[\text{HB}(2H\text{-benz}[g]\text{indazol-2-yl})_3]$  was ascribed to the indazole being coordinated to boron via the  $\text{N}^2$  rather than  $\text{N}^1$  nitrogen atom.<sup>7</sup> In contrast to these examples where enhanced coupling has been attributed to the proximity of thallium to the nucleus in question, the *absence* of thallium coupling in certain  $\text{Tl}[\text{Tp}^{\text{RR}'}]$  derivatives has been rationalized by *two* quite distinct explanations. Specifically, the absence of thallium coupling in some complexes has been interpreted as indicating structures which result in substituents being made distant from the thallium center,<sup>14</sup> while for other complexes the absence of thallium coupling has been proposed to be due to facile thallium dissociation.<sup>8,15,16</sup> In this paper, we report further on the interpretation of apparent  $J_{\text{Tl-H}}$  and  $J_{\text{Tl-C}}$  coupling constants<sup>17</sup> in  $\text{Tl}[\text{Tp}^{\text{RR}'}]$  derivatives, and describe how these values are

<sup>†</sup> Former address: University of the Virgin Islands, St. Thomas, U.S. Virgin Islands 00802. Present address: Symyx Technologies, 3100 Central Expressway, Santa Clara, CA 95051.

(1) For recent reviews, see: (a) Trofimenko, S. *Chem. Rev.* **1993**, *93*, 943–980. (b) Parkin, G. *Adv. Inorg. Chem.* **1995**, *42*, 291–393. (c) Kitajima, N.; Tolman, W. B. *Prog. Inorg. Chem.* **1995**, *43*, 419–531. (d) Santos, I.; Marques, N. *New J. Chem.* **1995**, *19*, 551–571. (e) Reger, D. L. *Coord. Chem. Rev.* **1996**, *147*, 571–595. (f) Etienne, M. *Coord. Chem. Rev.* **1997**, *156*, 201–236. (g) Byers, P. K.; Canty, A. J.; Honeyman, R. T. *Adv. Organomet. Chem.* **1992**, *34*, 1–65.

(2) The abbreviations adopted here for bis- and tris(pyrazolyl)hydroborato ligands are based on those described by Trofimenko (ref 1a). Thus, the tris(pyrazolyl)hydroborato ligands are represented by the abbreviation [Tp] with the 3- and 5-alkyl substituents listed respectively as superscripts. Likewise, bis(pyrazolyl)hydroborato ligands are represented by the abbreviation [Bp] with the appropriate superscripts.

(3) For reviews of  $\text{Tl}[\text{Tp}^{\text{RR}'}]$  complexes, see: (a) Janiak, C. *Main Group Metal Chem.* **1998**, *21*, 33–49. (b) Janiak, C. *Coord. Chem. Rev.* **1997**, *163*, 107–316.

(4) Trofimenko, S.; Calabrese, J. C.; Kochi, J. K.; Wolowicz, S.; Hulsbergen, F. B.; Reedijk, J. *Inorg. Chem.* **1992**, *31*, 3943–3950.

(5) Calabrese, J. C.; Trofimenko, S. *Inorg. Chem.* **1992**, *31*, 4810–4814.

(6) Rheingold, A. L.; Ostrander, R. L.; Haggerty, B. S.; Trofimenko, S. *Inorg. Chem.* **1994**, *33*, 3666–3676.

(7) Rheingold, A. L.; Haggerty, B. S.; Trofimenko, S. *J. Chem. Soc., Chem. Commun.* **1994**, 1973–1974.

(8) Rheingold, A. L.; Liabe-Sands, L. M.; Yap, G. P. A.; Trofimenko, S. *J. Chem. Soc., Chem. Commun.* **1996**, 1233–1234.

(9) LeCloux, D. D.; Tokar, C. J.; Osawa, M.; Houser, R. P.; Keyes, M. C.; Tolman, W. B. *Organometallics* **1994**, *13*, 2855–2866.

(10) Sanz, D.; Claramunt, R. M.; Glaser, J.; Trofimenko, S.; Elguero, J. *Magn. Reson. Chem.* **1996**, *34*, 843–846.

(11) For a compilation of  $J_{\text{Tl-C}}$  coupling constants in  $\text{Tl}[\text{Tp}^{\text{RR}'}]$  complexes, see: López, C.; Sanz, D.; Claramunt, R. M.; Trofimenko, S.; Elguero, J. *J. Organomet. Chem.* **1995**, *503*, 265–276.

(12) (a) Trofimenko, S.; Calabrese, J. C.; Thompson, J. S. *Inorg. Chem.* **1987**, *26*, 1507–1514. (b) Cowley, A. H.; Geerts, R. L.; Nunn, C. M.; Trofimenko, S. *J. Organomet. Chem.* **1989**, *365*, 19–22.

(13) It should be noted that subsequent X-ray diffraction studies indicate that the  $\text{Bu}^t$  groups of  $\text{Tl}[\text{Tp}^{\text{Bu}^t, \text{Me}}]$  are not appreciably closer to the Tl center than are the  $\text{Bu}^t$  groups of  $\text{Tl}[\text{Tp}^{\text{Bu}^t}]$ . For example, the average nonbonded  $\text{Tl} \cdots \text{CMe}_3$  distance in  $\text{Tl}[\text{Tp}^{\text{Bu}^t, \text{Me}}]$  is 3.96 Å,<sup>13a</sup> compared to 4.06 Å for  $\text{Tl}[\text{Tp}^{\text{Bu}^t}]$ .<sup>12b</sup> (a) Yoon, K.; Parkin, G. *Polyhedron* **1995**, *14*, 811–821.

(14) For example, the lack of observable coupling in  $\text{Tl}[\text{HB}(1,4\text{-dihydroindeno}[1,2-c]\text{pyrazol-1-yl})]$  as compared to  $\text{Tl}[\text{HB}(2H\text{-benz}[g]\text{-4,5-dihydroindazol-2-yl})_3]$  has been attributed to a shorter methylene tether in the former compound pulling the substituents away from the thallium center. See ref 6.

(15) Experimental data are, however, generally not provided to distinguish between these two possibilities.

strongly influenced by a mechanism that has not previously been recognized for such complexes. Specifically, the observed  $J_{\text{Tl-H}}$  and  $J_{\text{Tl-C}}$  coupling constants in these complexes are strongly influenced by rapid relaxation of the thallium nucleus via a mechanism that is a result of the large chemical shift anisotropy of thallium. As a consequence, the observed  $J_{\text{Tl-H}}$  and  $J_{\text{Tl-C}}$  coupling constants are highly dependent upon both (i) the magnitude of the spectrometer magnetic field strength and (ii) the sample temperature, such that considerable care must be exercised when using observed  $J_{\text{Tl-H}}$  and  $J_{\text{Tl-C}}$  coupling constants to infer differences in the structures and dynamics of  $\text{Tl}[\text{Tp}^{\text{RR}'}]$  complexes.

## Results and Discussion

Thallium, as both its  $^{203}\text{Tl}$  and  $^{205}\text{Tl}$  isotopes,<sup>18</sup> is renowned for exhibiting large  $^nJ_{\text{Tl-X}}$  coupling constants with other nuclei. In fact,  $^nJ_{\text{Tl-X}}$  coupling constants are among the largest reported,<sup>19</sup> with a value of 6144 Hz having been predicted for  $^1J_{\text{Tl-H}}$  of  $[\text{TlH}_4]^-$ .<sup>20</sup> Tris(pyrazolyl)hydroborato thallium complexes,  $\text{Tl}[\text{Tp}^{\text{RR}'}]$ , likewise exhibit substantial  $^nJ_{\text{Tl-H}}$  and  $^nJ_{\text{Tl-C}}$  coupling constants.<sup>1,11</sup> For example, the room temperature 200 MHz  $^1\text{H}$  NMR spectrum of the tris(3-*tert*-butylpyrazolyl)-hydroborato complex  $\text{Tl}[\text{Tp}^{\text{Bu}'}]$  is characterized by a long-range  $J_{\text{Tl-H}}$  coupling constant of 14.4 Hz with the hydrogen atoms of the *tert*-butyl groups. Most interestingly, however, the observed  $J_{\text{Tl-H}}$  coupling constants for  $\text{Tl}[\text{Tp}^{\text{Bu}'}]$  are significantly reduced upon recording the spectra at higher magnetic field strengths, with the result that *none* of the signals exhibit coupling in the room temperature 500 MHz  $^1\text{H}$  NMR spectrum (see Table 1 and Figures 2–4). Furthermore, the observed  $J_{\text{Tl-C}}$  coupling constants are also reduced upon increasing the magnetic field strength (Table 2), albeit to a lesser degree than observed for  $J_{\text{Tl-H}}$ .<sup>21</sup> It is, however, important to emphasize that the *true*  $J_{\text{Tl-X}}$  coupling constants themselves are not reduced; rather, it is the apparent coupling constants (i.e. the line separations) that are reduced.<sup>17</sup>

(16) Interestingly, two previous independent reports on  $\text{Tl}[\text{Tp}^{\text{Bu}'}]$  describe systematically different  $J_{\text{Tl-C}}$  coupling constants.

C(CH <sub>3</sub> ) <sub>3</sub>	C-3	C-4	ref
171	51	14	12b
175	66	39	11

It was suggested that the systematic discrepancy was due to the initial measurements being made "closer to the coalescence temperature".<sup>11</sup> However, since both spectra were recorded at the same temperature (298 K) in the same solvent ( $\text{CDCl}_3$ ), it is not clear that this provides a satisfactory explanation for the discrepancy. The data reported in this paper are more consistent with those of ref 11 and our temperature and magnetic field dependent studies provide no explanation for the data of ref 12b.

(17) In this article, we use the terms "apparent" and "observed" with respect to coupling constants to indicate that the values reported are merely the frequency separation of the multiplet components, recognizing that these values may be reduced from the true values due to the mechanisms described herein.

(18) Thallium exists as two naturally occurring spin  $1/2$  isotopes:  $^{203}\text{Tl}$  (29.5%,  $\gamma = 1.554 \times 10^8 \text{ rad T}^{-1} \text{ s}^{-1}$ ) and  $^{205}\text{Tl}$  (70.5%,  $\gamma = 1.569 \times 10^8 \text{ rad T}^{-1} \text{ s}^{-1}$ ). Due to the similarity of their gyromagnetic ratios, the difference in  $^{203}\text{Tl}$  and  $^{205}\text{Tl}$  coupling constants is generally not discernible [ $(J_{\text{Tl-X}}^{205}) = 1.0097(J_{\text{Tl-X}}^{203})$ ]. Likewise,  $^{203}\text{Tl}$  and  $^{205}\text{Tl}$  relaxation rates are very similar [ $R(^{205}\text{Tl}) = 1.0195 R(^{203}\text{Tl})$ ]. As such, the observed NMR phenomena for molecules containing  $^{203}\text{Tl}$  are essentially the same as those containing  $^{205}\text{Tl}$  so that corrections for isotopic content may be ignored.

(19) (a) Hinton, J. F. *Magn. Reson. Chem.* **1987**, 25, 659–669. (b) Hinton, J. F.; Metz, K. R.; Briggs, R. W. *Prog. NMR Spectrosc.* **1988**, 20, 423–513. (c) Hinton, J. F.; Metz, K. R. *NMR Newly Accessible Nucl.* **1983**, 2, 367–385. (d) Hinton, J. F.; Metz, K. R.; Briggs, R. W. *Annu. Rep. NMR Spectrosc.* **1982**, 13, 211–318.

(20) Tarasov, V. P.; Bakum, S. I. *J. Magn. Reson.* **1975**, 18, 64–68.

(21) The magnetic field effect on observed  $J_{\text{Tl-C}}$  coupling constants is less than that for  $J_{\text{Tl-H}}$  coupling constants due to the fact that their greater magnitude requires a greater  $^{203}\text{Tl}$  relaxation rate to effect decoupling.

**Table 1.**  $J_{\text{Tl-H}}$  Coupling Constant Data for  $\text{Tl}[\text{Tp}^{\text{Bu}'}]$  as a Function of Magnetic Field at Room Temperature in  $\text{CDCl}_3$ <sup>a</sup>

spectrometer freq/MHz	$J_{\text{Tl-H}}/\text{Hz}$		
	[C(CH <sub>3</sub> ) <sub>3</sub> ]	[H-4]	[H-5]
200 [4.70 T]	14.4	17.2	4.4
300 [7.05 T]	12.5	16.0	0
400 [9.40 T]	5.0	10.0	0
500 [11.75 T]	0	0	0

<sup>a</sup> Assignments taken from ref 12b.

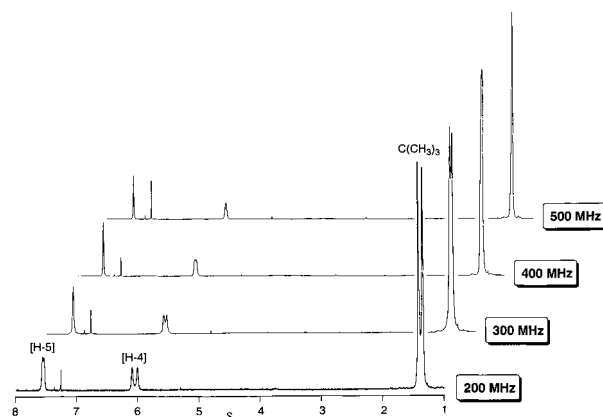


**Figure 2.** 200, 300, 400 and 500 MHz  $^1\text{H}$  NMR spectra of  $\text{Tl}[\text{Tp}^{\text{Bu}'}]$  in  $\text{CDCl}_3$  at room temperature.

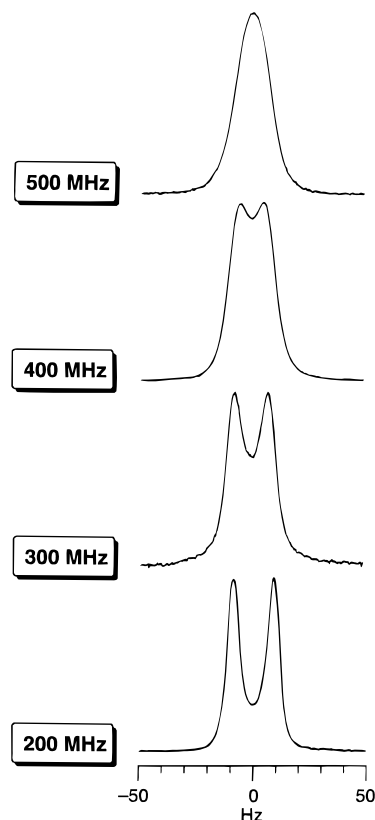


**Figure 3.** Magnetic field dependence of the [H-4] resonance of the  $\text{Tl}[\text{Tp}^{\text{Bu}'}]$  in  $\text{CDCl}_3$  at room temperature.

In addition to the above magnetic field strength dependence of the coupling constants, a strong temperature dependence is observed. Specifically, the  $J_{\text{Tl-H}}$  and  $J_{\text{Tl-C}}$  coupling constants are a maximum close to room temperature and decrease upon both lowering and raising the temperature from room temperature, as illustrated in Figures 5–7 and Tables 3–5. For example, at 300 MHz, the resonance attributable to H-4 exhibits

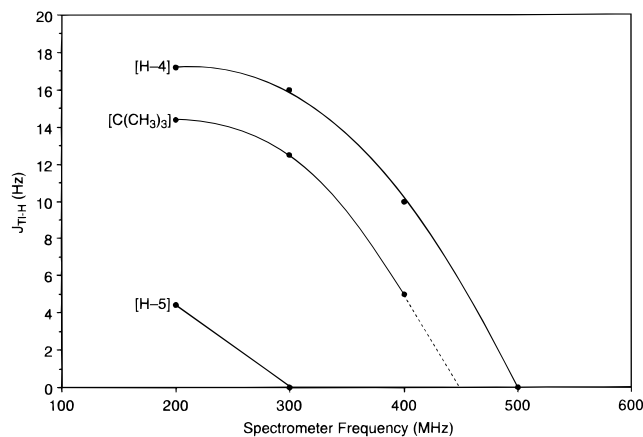


**Figure 4.** Magnetic field dependence of  $J_{\text{Tl-H}}$  coupling constants for  $\text{Tl}[\text{Tp}^{\text{Bu}^t}]$ .

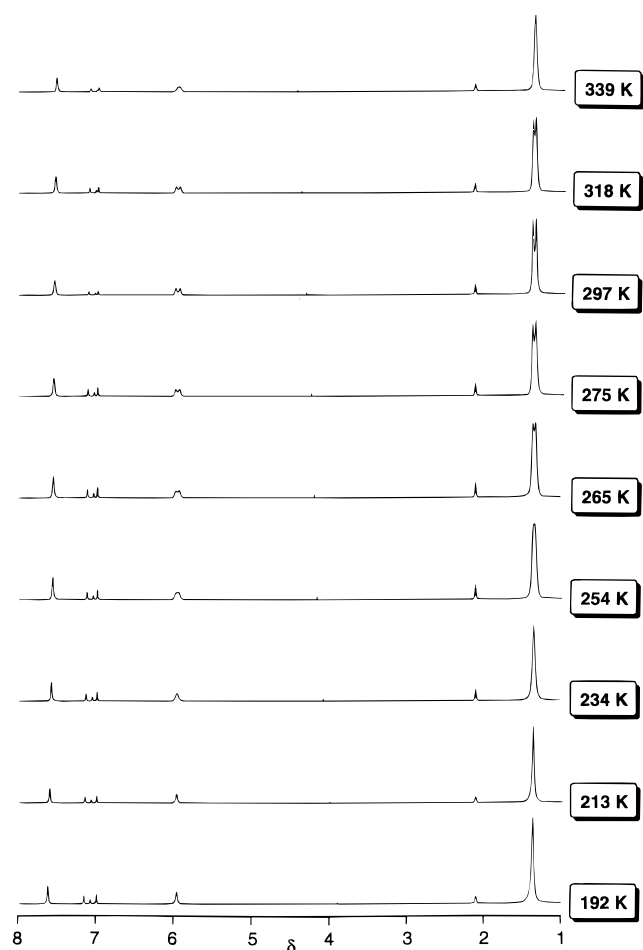


**Figure 5.** Variable-temperature 300 MHz  $^1\text{H}$  NMR spectra of  $\text{Tl}[\text{Tp}^{\text{Bu}^t}]$  in  $d_8$ -toluene.

**Table 2.**  $J_{\text{Tl-C}}$  Coupling Constant Data for  $\text{Tl}[\text{Tp}^{\text{Bu}^t}]$  as a Function of Magnetic Field at Room Temperature in  $\text{CDCl}_3^a$

spectrometer freq/MHz	$J_{\text{Tl-C}}/\text{Hz}$				
	$[\text{C}(\text{CH}_3)_3]$	$[\text{C}(\text{CH}_3)]$	[C-3]	[C-4]	[C-5]
49.7 [4.70 T] <sup>b</sup>	175		66	39	
75.5 [7.05 T]	175.0	16.2	67.2	43.2	15.5
100.6 [9.40 T]	175.0	0	67.0	38.8	0
125.8 [11.75 T]	174	0	65	37	0

<sup>a</sup> Assignments taken from ref 12b. <sup>b</sup> Data taken from ref 11.

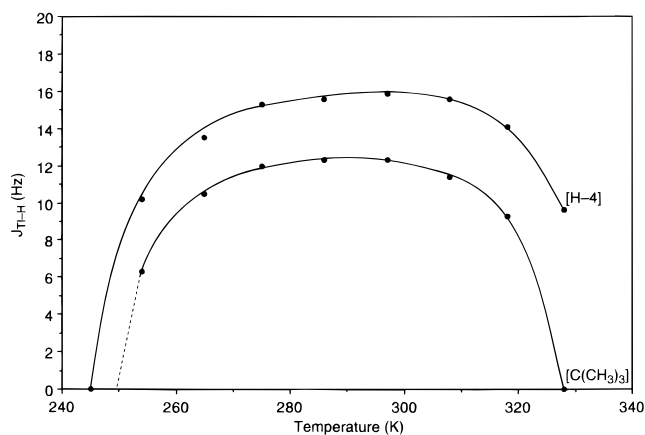


**Figure 6.** Temperature dependence of observed  $J_{\text{Tl-H}}$  coupling constants of  $\text{Tl}[\text{Tp}^{\text{Bu}^t}]$  in  $\text{CDCl}_3$  at 300 MHz (7.05 T).

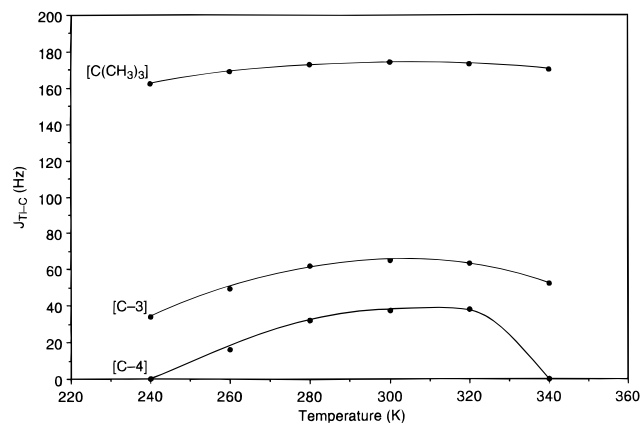


**Figure 7.** Temperature dependence of observed  $J_{\text{Tl-C}}$  coupling constants of  $\text{Tl}[\text{Tp}^{\text{Bu}^t}]$  in  $\text{CDCl}_3$  at 125.8 MHz (7.05 T).

**Table 3.** Temperature Dependence of  $J_{\text{Tl-H}}$  Coupling Constants for  $\text{Tl}[\text{Tp}^{\text{Bu}^t}]$  at 300 MHz in  $\text{CDCl}_3$  (values in parentheses for  $d_8$ -toluene)

$T/\text{K}$	$J_{\text{Tl-H}}/\text{Hz}$	
	$[\text{C}(\text{CH}_3)_3]$	[H-4]
245	0	0
254	6.3 (4.8)	10.2 (7.7)
265	10.5 (10.2)	13.5 (13.2)
275	12.0 (12.3)	15.3 (15.0)
286	12.3	15.6
297	12.3 (12.9)	15.9 (16.2)
308	11.4	15.6
318	9.3 (10.8)	14.1 (15.0)
328	0	9.6

**Table 4.** Temperature Dependence of  $J_{\text{Tl-C}}$  Coupling Constants for  $\text{Tl}[\text{Tp}^{\text{Bu}^t}]$  at 75.5 MHz in  $\text{CDCl}_3$

$T/\text{K}$	$J_{\text{Tl-C}}/\text{Hz}$				
	$[\text{C}(\text{CH}_3)_3]$	$[\text{C}(\text{CH}_3)]$	[C-3]	[C-4]	[C5]
214	172.3	0	55.1	21.8	0
254	174.7	8.5	65.5	40.5	8.9
297	175.0	16.2	67.2	43.2	15.5
339	173.3	0	59.1	36.8	0

a  $J_{\text{Tl-H}}$  coupling constant of ca. 16 Hz at room temperature, which is reduced to 0 Hz upon cooling to 245 K and is reduced to ca. 10 Hz upon warming to 328 K. These observations can be most easily explained by the existence of two independent processes with opposing temperature dependencies. As will be described in more detail below, the two opposing mechanisms

**Table 5.** Temperature Dependence of  $J_{\text{Tl}-\text{C}}$  Coupling Constants for  $\text{Tl}[\text{Tp}^{\text{Bu}}]$  at 125.8 MHz in  $\text{CDCl}_3$ 

T/K	$J_{\text{Tl}-\text{C}}/\text{Hz}$				
	$[\text{C}(\text{CH}_3)_3]$	$[\text{C}(\text{CH}_3)_3]$	[C-3]	[C-4]	[C5]
240	162	0	34	0	0
260	169	0	49	16	0
280	173	0	62	32	0
300	174	0	65	37	0
320	173	0	63	38	0
340	170	0	52	0	0

**Table 6.**  $^{203}\text{Tl}$   $T_1$  Relaxation Times at Room Temperature for  $\text{Tl}[\text{Tp}^{\text{Bu}}]$  as a Function of Magnetic Field Strength

$^{203}\text{Tl}$ $T_1/\text{ms}$	$^{203}\text{Tl}$ $(1/T_1)/\text{s}^{-1}$	$B_0^2/T^2$
34.4	29.1	49.703
18.0	55.6	88.172

responsible for the observed behavior are (i) thallium nuclear relaxation due to chemical shift anisotropy, which results in observed  $J_{\text{Tl}-\text{X}}$  coupling constants *increasing* with increasing temperature, and (ii) facile, reversible, thallium dissociation which results in observed  $J_{\text{Tl}-\text{X}}$  coupling constants *decreasing* with increasing temperature. The former mechanism dominates at low temperatures, while the latter mechanism dominates at high temperatures.

For many nuclei, e.g.  $^1\text{H}$ , the chemical shift range is sufficiently small that the chemical shift anisotropy is incapable of providing a significant contribution to the spin–lattice relaxation. However, for nuclei that exhibit large chemical shift ranges, the magnitude of the anisotropy may be such that the modulation of the magnetic field at a nucleus due to random tumbling at the Larmor frequency ( $\omega_0$ ) provides an efficient mechanism to effect spin–lattice relaxation (eq 1).<sup>22</sup> Representative examples of nuclei for which chemical shift anisotropy is known to provide an important contribution to relaxation include  $^{31}\text{P}$ ,<sup>23</sup>  $^{77}\text{Se}$ ,<sup>24</sup>  $^{57}\text{Fe}$ ,<sup>25</sup>  $^{103}\text{Rh}$ ,<sup>26</sup>  $^{195}\text{Pt}$ ,<sup>27</sup>  $^{207}\text{Pb}$ ,<sup>28</sup>  $^{199}\text{Hg}$ ,<sup>29</sup> and  $^{205}\text{Tl}$ .<sup>30</sup>

Decisive evidence for rapid relaxation of thallium due to chemical shift anisotropy contributing to the changes in  $J_{\text{Tl}-\text{H}}$  and  $J_{\text{Tl}-\text{C}}$  coupling constants for  $\text{Tl}[\text{Tp}^{\text{Bu}}]$  was obtained by

(22) (a) Farrar T. C.; Becker, E. D. *Pulse and FT NMR*; Academic Press: New York, 1971. (b) Farrar, T. C. *Introduction to Pulse NMR Spectroscopy*; The Farragut Press Chicago: Madison, 1989. (c) Thouvenot, R. *L'Actualité Chim.* **1996**, 7, 102–111.

(23) Randall, L. H.; Carty, A. A. *J. Inorg. Chem.* **1989**, 28, 1194–1196.

(24) Wong, T. C.; Ang, T. T.; Guziec, F. S., Jr.; Moustakis, C. A. *J. Magn. Reson.* **1984**, 57, 463–470.

(25) Baltzer, L.; Becker, E. D.; Averill, B. A.; Hutchinson, J. M.; Gansow, O. A. *J. Am. Chem. Soc.* **1984**, 106, 2444–2446.

(26) (a) Socol, S. M.; Meek, D. W. *Inorg. Chim. Acta* **1985**, 101, L45–L46. (b) Cocivera, M.; Ferguson, G.; Lenkinski, R. E.; Szczecinski, P.; Lalor, F. J.; O'Sullivan, D. J. *J. Magn. Reson.* **1982**, 46, 168–171.

(27) (a) Lallemand, J.-Y.; Soulié, J.; Chottard, J.-C. *J. Chem. Soc., Chem. Commun.* **1980**, 436–438. (b) Anklin, C. G.; Pregosin, P. S. *Magn. Reson. Chem.* **1985**, 23, 671–675. (c) Benn, R.; Büch, H. M.; Reinhardt, R.-D. *Magn. Reson. Chem.* **1985**, 23, 559–564. (d) Dechter, J. J.; Kowaleski, J. *J. Magn. Reson.* **1984**, 59, 146–149. (e) Pregosin, P. S. *Coord. Chem. Rev.* **1982**, 44, 247–291. (f) Ismail, I. M.; Kerrison, S. J. S.; Sadler, P. J. *Polyhedron* **1982**, 1, 57–59.

(28) (a) Hawk, R. M.; Sharp, P. R. *J. Chem. Phys.* **1974**, 60, 1522–1527. (b) Hays, G. R.; Gillies, D. G.; Blaauw, L. P.; Clague, A. D. H. *J. Magn. Reson.* **1981**, 45, 102–107.

(29) (a) Benn, R.; Günther, H.; Maercker, A.; Menger, V.; Schmitt, P. *Angew. Chem. Int. Ed. Engl.* **1982**, 21, 295–296. (b) Gillies, D. G.; Blaauw, L. P.; Hays, G. R.; Huis, R.; Clague, A. D. H. *J. Magn. Reson.* **1981**, 42, 420–428.

(30) (a) Brady, F.; Matthews, R. W.; Forster, M. J.; Gillies, D. G. *Inorg. Nucl. Chem. Lett.* **1981**, 17, 155–159. (b) Hinton, J. F.; Ladner, K. H. *J. Magn. Reson.* **1978**, 32, 303–306. (c) Brady, F.; Matthews, R. W.; Forster, M. J.; Gillies, D. G. *J. Chem. Soc., Chem. Commun.* **1981**, 911–912.

**Chart 1**

$$R(\text{CSA}) = \frac{1}{T_1(\text{CSA})} = (2/15)\gamma^2 B_0^2 (\sigma_{\parallel} - \sigma_{\perp})^2 \left\{ \frac{\tau_c}{1 + \omega_0^2 \tau_c^2} \right\} \quad (1)$$

$$\tau_c = \tau_c \exp(E_a/RT) \quad (2)$$

$$R(\text{CSA}) = \frac{1}{T_1(\text{CSA})} = (2/15)\gamma^2 B_0^2 (\sigma_{\parallel} - \sigma_{\perp})^2 \left\{ \frac{1}{\omega_0^2 \tau_c} \right\} \text{ for } \omega_0 \tau_c \gg 1 \quad (3)$$

$$R(\text{CSA}) = \frac{1}{T_1(\text{CSA})} = (2/15)\gamma^2 B_0^2 (\sigma_{\parallel} - \sigma_{\perp})^2 \tau_c \text{ for } \omega_0 \tau_c \ll 1 \quad (4)$$

$$R(\text{CSA}) = \frac{1}{T_1(\text{CSA})} = (2/15)\gamma^2 B_0^2 (\sigma_{\parallel} - \sigma_{\perp})^2 \left\{ \frac{\tau_c \exp(E_a/RT)}{1 + \omega_0^2 [\tau_c \exp(E_a/RT)]^2} \right\} \quad (5)$$

$$R(\text{DD}) = \frac{1}{T_1(\text{DD})} = \frac{3\gamma^4 r^6}{40\pi^2} \left\{ \frac{\tau_c \exp(E_a/RT)}{1 + \omega_0^2 [\tau_c \exp(E_a/RT)]^2} + \frac{4\tau_c \exp(E_a/RT)}{1 + 4\omega_0^2 [\tau_c \exp(E_a/RT)]^2} \right\} \quad (6)$$

$T_1(\text{CSA})$  = spin-lattice relaxation contribution from chemical shift anisotropy;  $\gamma$  = gyromagnetic ratio;  $B_0$  = applied magnetic field;  $\sigma_{\parallel}$  and  $\sigma_{\perp}$  = parallel and perpendicular components of the shielding tensor;  $\tau_c$  = rotational correlation time;  $\omega_0$  = Larmor frequency;  $T_1(\text{DD})$  = dipole-dipole contribution to spin-lattice relaxation;  $r$  = internuclear separation.

**Table 7.**  $^{203}\text{Tl}$  and  $^1\text{H}$   $T_1$  Relaxation Times for  $\text{Tl}[\text{Tp}^{\text{Bu}}]$  in  $\text{CDCl}_3$ 

T/K	$^{203}\text{Tl}$ $T_1/\text{ms}$	$^{203}\text{Tl}$ $(1/T_1)/\text{s}^{-1}$	$T_1/\text{s}$		
			$^1\text{H}[\text{C}(\text{CH}_3)_3]$	$^1\text{H}[\text{H}-4]$	$^1\text{H}[\text{H}-5]$
214	5.9	170	0.368	1.41	1.06
254	15.9	63	0.775	2.42	1.74
297	34.4	29	1.64	4.43	3.39
339	58.2	17	2.86	7.39	5.88

measuring the magnetic field strength dependence of the  $^{203}\text{Tl}$  spin–lattice relaxation time.<sup>31</sup> Thus, at room temperature, the  $^{203}\text{Tl}$  relaxation rate ( $R = 1/T_1$ ) increases dramatically with magnetic field strength (Table 6), with a magnitude that is consistent with the observed decrease in coupling constants.<sup>30c</sup> This magnetic field strength dependence of the  $^{203}\text{Tl}$  relaxation rate strongly implicates chemical shift anisotropy as the source of the relaxation since, unlike all other mechanisms of relaxation, which are either field independent or vary inversely with field strength,<sup>32</sup> relaxation due to chemical shift anisotropy increases with magnetic field strength in the extreme narrowing limit ( $\omega_0 \tau_c \ll 1$ ).<sup>22</sup> Specifically, the relaxation rate due to chemical shift anisotropy for axially symmetric molecules depends on the magnetic field strength, the rotational correlation time, and the chemical shift anisotropy (eq 1). The rotational correlation time,  $\tau_c$ , is a function of temperature (eq 2), and at low temperatures the condition  $\omega_0 \tau_c \gg 1$  is satisfied. Under this condition, the relaxation rate (eq 3) is independent of  $B_0$  (since  $\omega_0 = -\gamma B_0$ ) and increases with increasing temperature. At high temperatures, the condition  $\omega_0 \tau_c \ll 1$  is satisfied, such that the relaxation rate is directly proportional to  $B_0^2$  (eq 4) and decreases with increasing temperature. Since the observed decrease in  $R$  with increasing temperature (Table 7) identifies these experiments as being carried out in the high-temperature regime, the observed field dependence of  $R$  (Table 6) is clear evidence that chemical shift anisotropy is the most significant contributor to thallium relaxation. Furthermore, it should be noted that short  $^{203}\text{Tl}$   $T_1$  relaxation times are also observed for other  $\text{Tl}[\text{Tp}^{\text{RR}'}]$  derivatives (Table 8), and so the effect is very likely to be general for this type of complex. The reduction in the observed  $J_{\text{Tl}-\text{H}}$  and  $J_{\text{Tl}-\text{C}}$  coupling constants for  $\text{Tl}[\text{Tp}^{\text{Bu}}]$  upon lowering the temperature from room temperature (Tables 3–5 and Figures 6–7) is,

(31)  $^{203}\text{Tl}$  NMR studies were carried out in preference to  $^{205}\text{Tl}$  NMR studies due to the greater sensitivity for  $^{203}\text{Tl}$  with the available probe.

(32) Other relaxation mechanisms include dipole–dipole, spin-rotation, electric quadrupole, and scalar relaxation, of which the lattermost exhibits an inverse  $1/B_0^2$  dependence. See: Howarth, O. In *Multinuclear NMR*; Mason, J., Ed.; Plenum Press: New York, 1987; Chapter 5.

**Table 8.**  $^{203}\text{Tl}$  Chemical Shift and  $T_1$  Relaxation Times at 171.4 MHz for Some  $\text{Ti}[\text{Tp}^{\text{RR}}]$  Complexes in  $\text{CDCl}_3$  at Room Temperature

	$\delta/\text{ppm}$	$T_1/\text{ms}$	MW
$\text{Ti}[\text{Tp}^{\text{Me}_2}]$	2208	33	503
$\text{Ti}[\text{Tp}^{\text{Bu}^t}]$	2021	33	616
$\text{Ti}[\text{Tp}^{\text{Bu}^t_2}]$	2135	21	754
$\text{Ti}[\text{Tp}^{\text{CF}_3, \text{Me}}]$	1284	47	664
$\text{Ti}[\text{Tp}^{\text{CF}_3, \text{Tn}}]$	1132	35	868
$\text{Ti}[\text{Tp}^{p\text{-Tol}}]$	1783	18	688
$\text{Ti}[\text{Tp}^{\text{Ar}_2}]^a$	1849	5	1211

<sup>a</sup> Ar = *p*-C<sub>6</sub>H<sub>4</sub>Bu<sup>t</sup>.**Table 9.**  $^{203}\text{Tl}$  Chemical Shift Anisotropy and Rotational Correlation Time Parameters for  $\text{Ti}[\text{Tp}^{\text{RR}}]$  Complexes Determined by  $^{203}\text{Tl}$  NMR Relaxation Studies

	$E_a/\text{kcal mol}^{-1}$	$\tau_0/\text{s}$	$(\sigma_{\parallel} - \sigma_{\perp})/\text{ppm}$
$\text{Ti}[\text{Tp}^{\text{Bu}^t}]$	2.66	$3.00 \times 10^{-13}$	2635
$\text{Ti}[\text{Tp}^{\text{Ar}_2}]$	2.58	$3.69 \times 10^{-12}$	2156
$\text{Ti}[\text{Tp}^{p\text{-Tol}}]$	2.47	$1.54 \times 10^{-12}$	2003

<sup>a</sup> Ar = *p*-C<sub>6</sub>H<sub>4</sub>Bu<sup>t</sup>.

therefore, a consequence of increased thallium relaxation at lower temperatures (Table 7 and Figure 8).

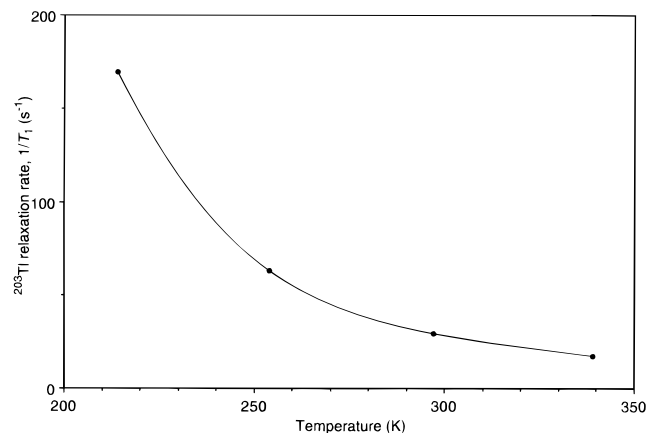
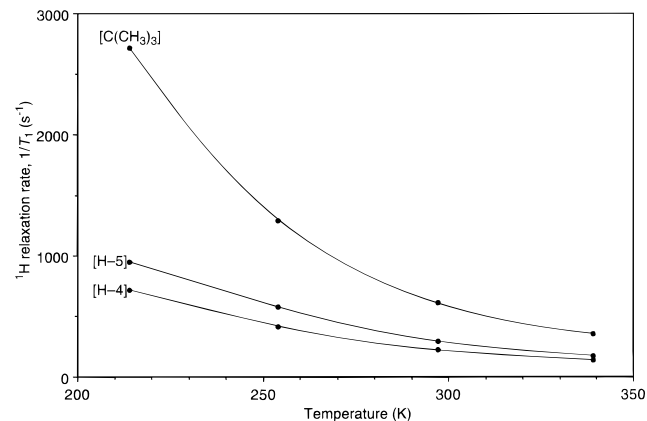
A detailed analysis of the temperature dependence of the  $^{203}\text{Tl}$  relaxation rate for  $\text{Ti}[\text{Tp}^{\text{Bu}^t}]$  has allowed an estimate of the magnitude of the chemical shift anisotropy ( $\sigma_{\parallel} - \sigma_{\perp}$ ) to be obtained. Specifically, expressing  $\tau_c$  as a function of temperature,  $\tau_c = \tau_0 \exp(E_a/RT)$ ,<sup>22</sup> the  $^{203}\text{Tl}$  relaxation rate (eq 1) becomes an explicit function of temperature (eq 5), and the experimental data ( $R$  and  $T$ ) for  $\text{Ti}[\text{Tp}^{\text{Bu}^t}]$  may be fit by treating ( $\sigma_{\parallel} - \sigma_{\perp}$ ),  $\tau_0$ , and  $E_a$  as adjustable parameters. The best fit values are listed in Table 9, which also includes for comparison the data for  $\text{Ti}[\text{Tp}^{p\text{-Tol}}]$ <sup>33</sup> and  $\text{Ti}[\text{Tp}^{\text{Ar}_2}]$  (Ar = *p*-C<sub>6</sub>H<sub>4</sub>Bu<sup>t</sup>),<sup>34</sup> respectively.<sup>35</sup> Support for the reliability of these data is provided by the fact that the values of  $E_a$ ,  $\tau_0$ , and ( $\sigma_{\parallel} - \sigma_{\perp}$ ) for  $\text{Ti}[\text{Tp}^{\text{Bu}^t}]$  are also consistent with the magnetic field strength dependence of the  $^{203}\text{Tl}$  relaxation rate (Table 6).<sup>36</sup> Thus, the observed slope of  $0.63 \text{ s}^{-1} \text{ T}^{-2}$  in the plot of  $R$  versus  $B_0^2$  compares favorably with the value of  $0.60 \text{ s}^{-1} \text{ T}^{-2}$  predicted by the expression  $(2/15)\gamma^2(\sigma_{\parallel} - \sigma_{\perp})^2\tau_0 \exp(E_a/RT)$  (eqs 2 and 4), using the values of  $E_a$ ,  $\tau_0$ , and ( $\sigma_{\parallel} - \sigma_{\perp}$ ) listed in Table 9. Finally, the values of  $E_a$  and  $\tau_0$  for  $\text{Ti}[\text{Tp}^{\text{Bu}^t}]$  obtained by analyzing  $^{203}\text{Tl}$  relaxation data (Table 9) are also comparable in magnitude to the values estimated by the temperature dependence of the  $^1\text{H}$   $T_1$  relaxation rates (Figure 9 and Table 10), assuming that dipole–dipole interactions are the major contributors to relaxation (eq 6).<sup>37</sup>

While the relaxation phenomenon due to chemical shift anisotropy convincingly explains the observed reduction in  $J_{\text{Ti-H}}$  and  $J_{\text{Ti-C}}$  coupling constants upon lowering the temperature

(33) Ferguson, G.; Jennings, M. C.; Lalor, F. J.; Shanahan, C. *Acta Crystallogr.* **1991**, C47, 2079–2082.(34) Libertini, E.; Yoon, K.; Parkin, G. *Polyhedron* **1993**, 12, 2539–2542.(35) The chemical shift anisotropy ( $\sigma_{\parallel} - \sigma_{\perp}$ ) for  $\text{Ti}[\text{Tp}^{\text{Ar}_2}]$  can also be calculated directly since the minimum value of  $T_1$  as a function of temperature could be measured (2.9 ms at 234 K). Specifically,  $\tau_c$  is known at the minimum *via* the relationship  $\tau_c = 1/\omega_0$ ,<sup>35a</sup> so that the chemical shift anisotropy ( $\sigma_{\parallel} - \sigma_{\perp}$ ) can be calculated directly from eq 1. The value obtained by this method, 2170 ppm, compares favorably with that of 2160 ppm listed in Table 9. (a) Equation 1 is a minimum when  $d/d\tau_c\{\tau_c/(1 + \tau_c^2\omega_0^2)\} = 0$ .(36) Furthermore, the  $^{203}\text{Tl}$  chemical shift anisotropy of  $\text{Ti}[\text{Tp}^{\text{Bu}^t}]$  has been estimated to be *ca.* 2000 ppm by solid-state NMR spectroscopy. McDermott, A.; Peshkovsky, A. Personal communication.(37) It should be noted that the motions responsible for relaxing thallium and hydrogen nuclei need not necessarily be the same, and so the  $E_a$  and  $\tau_0$  values for the different relaxation processes are not required to be identical.**Table 10.** Rotational Correlation Time Parameters for  $\text{Ti}[\text{Tp}^{\text{Bu}^t}]$  Determined by  $^1\text{H}$  NMR Relaxation Studies at 300 MHz

	$E_a/\text{kcal mol}^{-1}$	$\tau_0/\text{s}$	$r_{\text{eff}}/\text{\AA}^a$
H-4	2.69	$5.05 \times 10^{-13}$	2.27
H-5	2.42	$7.71 \times 10^{-13}$	2.36
$\text{C}(\text{CH}_3)_3$	2.77	$2.85 \times 10^{-13}$	1.87

<sup>a</sup>  $r_{\text{eff}}$  is a composite value for  $r$ , representing all dipolar contributions, in eq 6. For comparison, the closest H···H interactions are *ca.* 2.6 Å for the CH groups and 1.7 Å for the CH<sub>3</sub> groups.

**Figure 8.**  $^{203}\text{Tl}$  relaxation rates ( $1/T_1$ ) for  $\text{Ti}[\text{Tp}^{\text{Bu}^t}]$  at 171.4 MHz (7.05 T) in  $\text{CDCl}_3$  as a function of temperature.**Figure 9.**  $^1\text{H}$  relaxation rates ( $1/T_1$ ) for  $\text{Ti}[\text{Tp}^{\text{Bu}^t}]$  in  $\text{CDCl}_3$  as a function of temperature at 300 MHz.

from room temperature to *ca.* 220 K, it does not account for the decrease in coupling constant upon raising the temperature from room temperature, since the  $^{203}\text{Tl}$  spin–lattice relaxation rate continues to decrease (Table 7 and Figure 8). Consequently, another process must be invoked to rationalize the reduction in  $J_{\text{Ti-H}}$  and  $J_{\text{Ti-C}}$  coupling constants above this temperature. The most likely origin of the decrease in coupling constants above room temperature is thallium dissociation. Evidence supporting this proposal is provided by the observation of  $^{203}\text{Tl}$  magnetization transfer between  $\text{Ti}[\text{Tp}^{\text{Ar}_2}]$  (Ar = *p*-C<sub>6</sub>H<sub>4</sub>Bu<sup>t</sup>) and  $\text{Ti}[\text{Tp}^{p\text{-Tol}}]$ . Furthermore, the reduction in  $J_{\text{Ti-C}}$  coupling constants for  $\text{Ti}[\text{Tp}^{\text{Me}_2}]$  with increasing temperature has also been attributed to a dynamic process involving thallium dissociation.<sup>10</sup> Likewise, the highly solvent dependent nature of the  $^4J_{\text{Ti-F}}$  coupling constant (ranging from 850 to 0 Hz) for the tris[3-trifluoromethyl-5-(2-thienyl)pyrazolyl]hydroborato thallium complex,  $\text{Ti}[\text{Tp}^{\text{CF}_3, \text{Tn}}]$ , has been ascribed to thallium dissociation.<sup>38,39</sup>

(38) Han, R.; Ghosh, P.; Desrosiers, P. J.; Trofimenko, S.; Parkin, G. J. *Chem. Soc., Dalton Trans.* **1997**, 3713–3717.

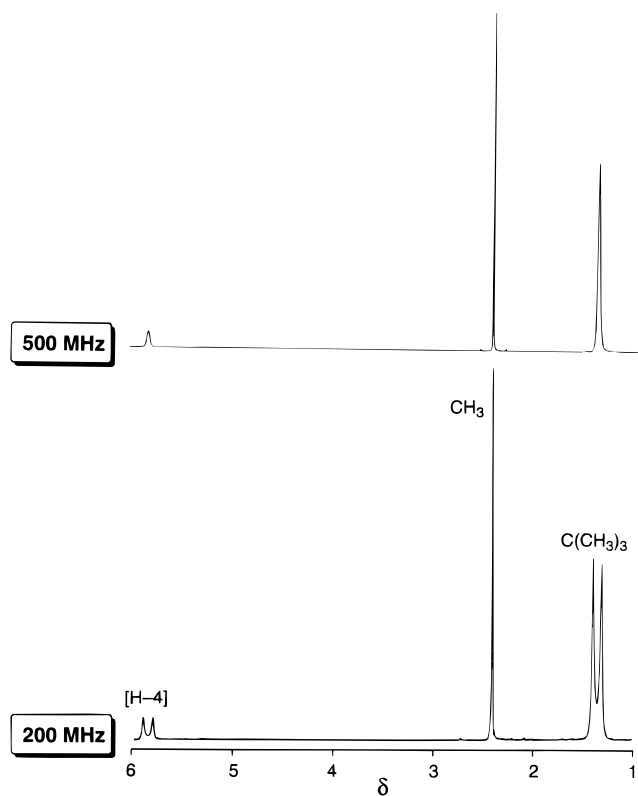


**Figure 10.** 200 and 500 MHz  $^1\text{H}$  NMR spectra of  $\text{Tl}[\text{Tp}^{\text{Bu}^t,\text{Me}}]$  in  $\text{CDCl}_3$  at room temperature.

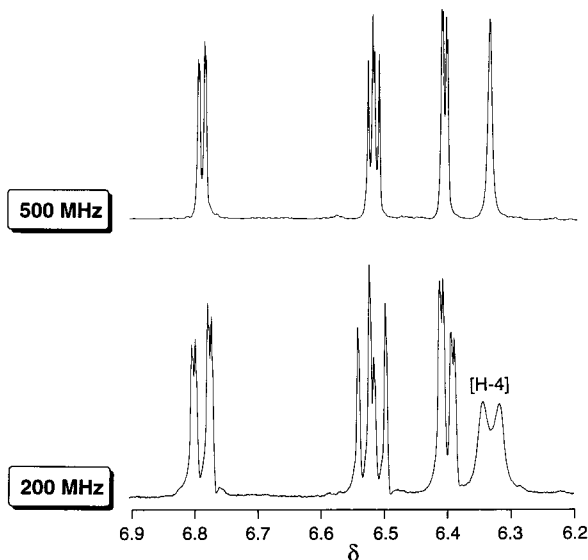


**Figure 11.** 200 and 500 MHz  $^1\text{H}$  NMR spectra of  $\text{Tl}[\text{Tp}^{\text{CF}_3,\text{Tn}}]$  in  $d_8$ -toluene at room temperature.

It is important to emphasize that the influence of thallium relaxation upon the  $^1\text{H}$  and  $^{13}\text{C}$  NMR spectra of  $\text{Tl}[\text{Tp}^{\text{RR}'}]$  derivatives is not limited to the example of  $\text{Tl}[\text{Tp}^{\text{Bu}^t}]$  described above. As an illustration, the magnetic field strength dependencies of the  $^1\text{H}$  NMR spectra of  $\text{Tl}[\text{Tp}^{\text{Bu}^t,\text{Me}}]$  and  $\text{Tl}[\text{Tp}^{\text{CF}_3,\text{Tn}}]$  are shown in Figures 10 and 11, respectively.

While it is certainly true that structural and dynamic factors may influence the  $^1\text{H}$  and  $^{13}\text{C}$  NMR spectra of  $\text{Tl}[\text{Tp}^{\text{RR}'}]$  derivatives, the examples described herein serve to demonstrate

(39) In addition, it has been noted that apparent  $J_{\text{Tl}-\text{C}}$  and  $J_{\text{Tl}-\text{H}}$  coupling constants for  $\text{Tl}[\text{Tp}^{\text{RR}'}]$  complexes may be solvent dependent. See: López, C.; Sanz, D.; Claramunt, R. M.; Trofimenko, S.; Elguero, J. J. *Organomet. Chem.* **1995**, *503*, 265–276.

that the spectra may also be strongly influenced by a nuclear relaxation phenomenon. Factors which influence the nuclear relaxation rate include the rotational correlation time ( $\tau_c$ ) and the chemical shift anisotropy ( $\sigma_{\parallel} - \sigma_{\perp}$ ). Since these are both inherent molecular properties (which are not expected to be the same for different complexes), it is evident that the effect of thallium relaxation on the  $^1\text{H}$  and  $^{13}\text{C}$  NMR spectra will be a unique property of the molecule in question. As such, the existence of this magnetic field strength and temperature-dependent phenomenon needs to be considered when using observed  $J_{\text{Tl}-\text{H}}$  and  $J_{\text{Tl}-\text{C}}$  coupling constant data to provide structural correlations between various molecules.<sup>40</sup> Likewise, the absence of thallium couplings does not necessarily indicate that dissociation is facile.

## Conclusion

In summary, the  $^1\text{H}$  and  $^{13}\text{C}$  NMR spectra of  $\text{Tl}[\text{Tp}^{\text{RR}'}]$  complexes provide exemplary illustrations of the effect of thallium chemical shift anisotropy. Specifically, chemical shift anisotropy provides an efficient mechanism to modulate apparent  $J_{\text{Tl}-\text{H}}$  and  $J_{\text{Tl}-\text{C}}$  coupling constants in  $\text{Tl}[\text{Tp}^{\text{RR}'}]$  complexes in such a manner that they are dramatically reduced at (i) higher applied magnetic field strengths and (ii) lower temperatures. As a result of this phenomenon, the absence of observable  $J_{\text{Tl}-\text{H}}$  and  $J_{\text{Tl}-\text{C}}$  coupling constants, per se, should not be taken as definitive evidence that either (i) the structure is static with a coupling constant of zero or (ii) dissociation of Tl is rapid on the NMR time scale, thereby resulting in an observed loss of coupling. Magnetic field strength and temperature-dependent studies are required to provide information to distinguish between the various possibilities.

## Experimental Section

$\text{Tl}[\text{Tp}^{\text{Me}_2}]$ ,<sup>41</sup>  $\text{Tl}[\text{Tp}^{\text{Bu}^t}]$ ,<sup>12a</sup>  $\text{Tl}[\text{Tp}^{\text{Bu}^t_2}]$ ,<sup>42</sup>  $\text{Tl}[\text{Tp}^{\text{p-Tol}}]$ ,<sup>33</sup> and  $\text{Tl}[\text{Tp}^{\text{Ar}_2}]$  ( $\text{Ar} = p\text{-C}_6\text{H}_4\text{Bu}^t$ )<sup>34</sup> were prepared by literature methods.  $\text{Tl}[\text{Tp}^{\text{CF}_3,\text{Me}}]$  and  $\text{Tl}[\text{Tp}^{\text{CF}_3,\text{Tn}}]$  were provided as generous gifts from Dr. C. Dowling (Elf Atochem) and Dr. S. Trofimenko (University of Delaware), respectively.

$^1\text{H}$  NMR spectra were recorded on Varian VXR 200, Bruker Avance 300wb DRX, Bruker Avance 400 DRX, and Bruker Avance 500 DMX spectrometers and are referenced relative to TMS, using residual protio solvent signals as an internal calibrant.  $^{13}\text{C}$  NMR spectra were recorded on Bruker Avance 300wb DRX (75.476 MHz), Bruker Avance 400 DRX (100.570 MHz), and Bruker Avance 500 DMX (125.774 MHz) spectrometers and are referenced relative to TMS, using solvent signals as an internal calibrant.  $^{203}\text{Tl}$  NMR spectra were recorded on Bruker Avance 300wb DRX (171.440 MHz) and Bruker Avance 400 DRX (228.587 MHz) spectrometers and are referenced relative to aqueous  $\text{TlNO}_3$  (extrapolated to infinite dilution;  $\delta$  0.00 ppm),<sup>43,44</sup> using an external solution of aqueous TlOAc as calibrant. In light of the large chemical shift range and rapid relaxation times for  $^{203}\text{Tl}$ , standard 1D

(40) In this regard, Tolman<sup>9</sup> has previously noted that  $J_{\text{Tl}-\text{C}}$  coupling constants in a series of  $\text{Tl}[\text{Tp}^{\text{RR}'}]$  complexes do not correlate in a simple fashion with distance between Tl and C, and has pointed out difficulties with interpreting structural features on the basis of  $J_{\text{Tl}-\text{C}}$  coupling constants; he has also questioned whether these couplings should be considered as operating “through-space”. “Through-space”<sup>40a-c</sup> couplings of thallium to other nuclei have, nevertheless, been previously postulated in other systems.<sup>40d,e</sup> (a) Petrakis, L.; Sederholm, C. H. *J. Chem. Phys.* **1961**, *35*, 1243–1248. (b) Ng, S.; Sederholm, C. H. *J. Chem. Phys.* **1964**, *40*, 2090–2094. (c) Hilton, J.; Sutcliffe, L. H. *Prog. Nucl. Magn. Reson. Spectrosc.* **1975**, *10*, 27–39. (d) Cheesman, B. V.; White, R. F. M. *Can. J. Chem.* **1984**, *62*, 521–525. (e) Pecksen, G. N.; White, R. F. M. *Can. J. Chem.* **1989**, *67*, 1847–1850.

(41) Trofimenko, S. *J. Am. Chem. Soc.* **1967**, *89*, 6288–6294.

(42) Dowling, C. M.; Leslie, D.; Chisholm, M. H.; Parkin, G. *Main Group Chem.* **1995**, *1*, 29–52.

(43) Dechter, J. J.; Zink, J. I. *J. Am. Chem. Soc.* **1975**, *97*, 2937–2942.

(44) Specifically, the resonance frequencies of three solutions of  $\text{Tl}(\text{NO}_3)$  in  $\text{H}_2\text{O}$  (1.0, 0.5, and 0.25 M) were extrapolated to zero concentration.

spectra were acquired with use of a large sweep width (150 000 Hz), short acquisition (<0.2 s) and delay (<0.1 s) times, and a 90° pulse width. However, even with this large sweep width (corresponding to ca. 800 ppm), due to the large  $^{203}\text{Tl}$  chemical shift range, it was often necessary to move the offset several times before the resonances could be found. The FIDs were subject to substantial exponential multiplication (line broadening factors of 50 to 500 Hz) before Fourier transformation.  $T_1$  measurements were made following the standard inversion recovery method. Although the line widths were often large (several hundred to a thousand hertz at half-height), therefore resulting in weak signals, the short relaxation times made it possible to acquire

hundreds of transients at each delay time within a matter of minutes. Typical  $T_1$  experiments used 16 different delay times ranging from 0.2 to 500 ms and required 30 to 60 min to complete.

**Acknowledgment.** We thank the National Science Foundation (CHE 96-10497) for support of this research and Professor Jack Norton, Professor Ann McDermott, and Dr. John Decatur for providing useful comments. G.P. is the recipient of a Presidential Faculty Fellowship Award (1992–1997).

JA981636H